

# Supplementary Materials for “Personalized Biopsies in Prostate Cancer Active Surveillance”

Anirudh Tomer, MSc<sup>a,\*</sup>, Daan Nieboer, MSc<sup>b</sup>, Monique J. Roobol, PhD<sup>c</sup>, Anders Bjartell, PhD<sup>d</sup>, Ewout W. Steyerberg, PhD<sup>b,e</sup>, Dimitris Rizopoulos, PhD<sup>a</sup>, Movember Foundations Global Action Plan Prostate Cancer Active Surveillance (GAP3) consortium<sup>f</sup>

<sup>a</sup>*Department of Biostatistics, Erasmus University Medical Center, Rotterdam, the Netherlands*

<sup>b</sup>*Department of Public Health, Erasmus University Medical Center, Rotterdam, the Netherlands*

<sup>c</sup>*Department of Urology, Erasmus University Medical Center, Rotterdam, the Netherlands*

<sup>d</sup>*Department of Urology, Skåne University Hospital, Malmö, Sweden*

<sup>e</sup>*Department of Biomedical Data Sciences, Leiden University Medical Center, Leiden, the Netherlands*

<sup>f</sup>*The Movember Foundations Global Action Plan Prostate Cancer Active Surveillance (GAP3) consortium members presented in Appendix A*

---

---

## 1 Appendix A. A Joint Model for the Longitudinal PSA, and Time 2 to Gleason Reclassification

3 Let  $T_i^*$  denote the true time of reclassification (increase in biopsy Gleason  
4 grade from 1 to 2 or higher) for the  $i$ -th patient included in PRIAS. Since  
5 biopsies are conducted periodically,  $T_i^*$  is observed with interval censoring  
6  $l_i < T_i^* \leq r_i$ . When reclassification is observed for the patient at his latest  
7 biopsy time  $r_i$ , then  $l_i$  denotes the time of the second latest biopsy. Oth-  
8 erwise,  $l_i$  denotes the time of the latest biopsy and  $r_i = \infty$ . Let  $\mathbf{y}_i$  denote

---

\*Corresponding author (Anirudh Tomer): Erasmus MC, kamer flex Na-2823, PO Box 2040, 3000 CA Rotterdam, the Netherlands. Tel: +31 10 70 43393

*Email addresses:* [a.tomer@erasmusmc.nl](mailto:a.tomer@erasmusmc.nl) (Anirudh Tomer, MSc),  
[d.nieboer@erasmusmc.nl](mailto:d.nieboer@erasmusmc.nl) (Daan Nieboer, MSc), [m.roobol@erasmusmc.nl](mailto:m.roobol@erasmusmc.nl) (Monique J. Roobol, PhD), [anders.bjartell@med.lu.se](mailto:anders.bjartell@med.lu.se) (Anders Bjartell, PhD),  
[e.w.steyerberg@lumc.nl](mailto:e.w.steyerberg@lumc.nl) (Ewout W. Steyerberg, PhD), [d.rizopoulos@erasmusmc.nl](mailto:d.rizopoulos@erasmusmc.nl) (Dimitris Rizopoulos, PhD)

his observed PSA longitudinal measurements. The observed data of all  $n$  patients is denoted by  $\mathcal{D}_n = \{l_i, r_i, \mathbf{y}_i; i = 1, \dots, n\}$ .

In our joint model, the patient-specific PSA measurements over time are modeled using a linear mixed effects sub-model. It is given by (see Panel A, Figure 1):

$$\begin{aligned} \log_2 \{y_i(t) + 1\} &= m_i(t) + \varepsilon_i(t), \\ m_i(t) &= \beta_0 + b_{0i} + \sum_{k=1}^4 (\beta_k + b_{ki}) B_k\left(\frac{t-2}{2}, \frac{\mathcal{K}-2}{2}\right) + \beta_5 \text{age}_i, \end{aligned} \quad (1)$$

where,  $m_i(t)$  denotes the measurement error free value of  $\log_2(\text{PSA} + 1)$  transformed [2, 3] measurements at time  $t$ . We model it non-linearly over time using B-splines [4]. To this end, our B-spline basis function  $B_k\{(t-2)/2, (\mathcal{K}-2)/2\}$  has 3 internal knots at  $\mathcal{K} = \{0.5, 1.3, 3\}$  years, which are the three quartiles of the observed follow-up times. The boundary knots of the spline are at 0 and 6.3 years (95-th percentile of the observed follow-up times). We mean centered (mean 2 years) and standardized (standard deviation 2 years) the follow-up time  $t$  and the knots of the B-spline  $\mathcal{K}$  during parameter estimation for better convergence. The fixed effect parameters are denoted by  $\{\beta_0, \dots, \beta_5\}$ , and  $\{b_{0i}, \dots, b_{4i}\}$  are the patient specific random effects. The random effects follow a multivariate normal distribution with mean zero and variance-covariance matrix  $\mathbf{D}$ . The error  $\varepsilon_i(t)$  is assumed to be t-distributed with three degrees of freedom (see Appendix B.1) and scale  $\sigma$ , and is independent of the random effects.

To model the impact of PSA measurements on the risk of reclassification, our joint model uses a relative risk sub-model. More specifically, the hazard of reclassification denoted as  $h_i(t)$ , and the cumulative risk of reclassification denoted as  $R_i(t)$ , at a time  $t$  are (see Panel C, Figure 1):

$$\begin{aligned} h_i(t) &= h_0(t) \exp\left(\gamma \text{age}_i + \alpha_1 m_i(t) + \alpha_2 \frac{\partial m_i(t)}{\partial t}\right), \\ R_i(t) &= \exp\left\{-\int_0^t h_i(s) ds\right\}, \end{aligned} \quad (2)$$

where,  $\gamma$  is the parameter for the effect of age. The impact of PSA on the hazard of reclassification is modeled in two ways, namely the impact of the error free underlying PSA value  $m_i(t)$  (see Panel A, Figure 1), and the impact of the underlying PSA velocity  $\partial m_i(t)/\partial t$  (see Panel B, Figure 1).

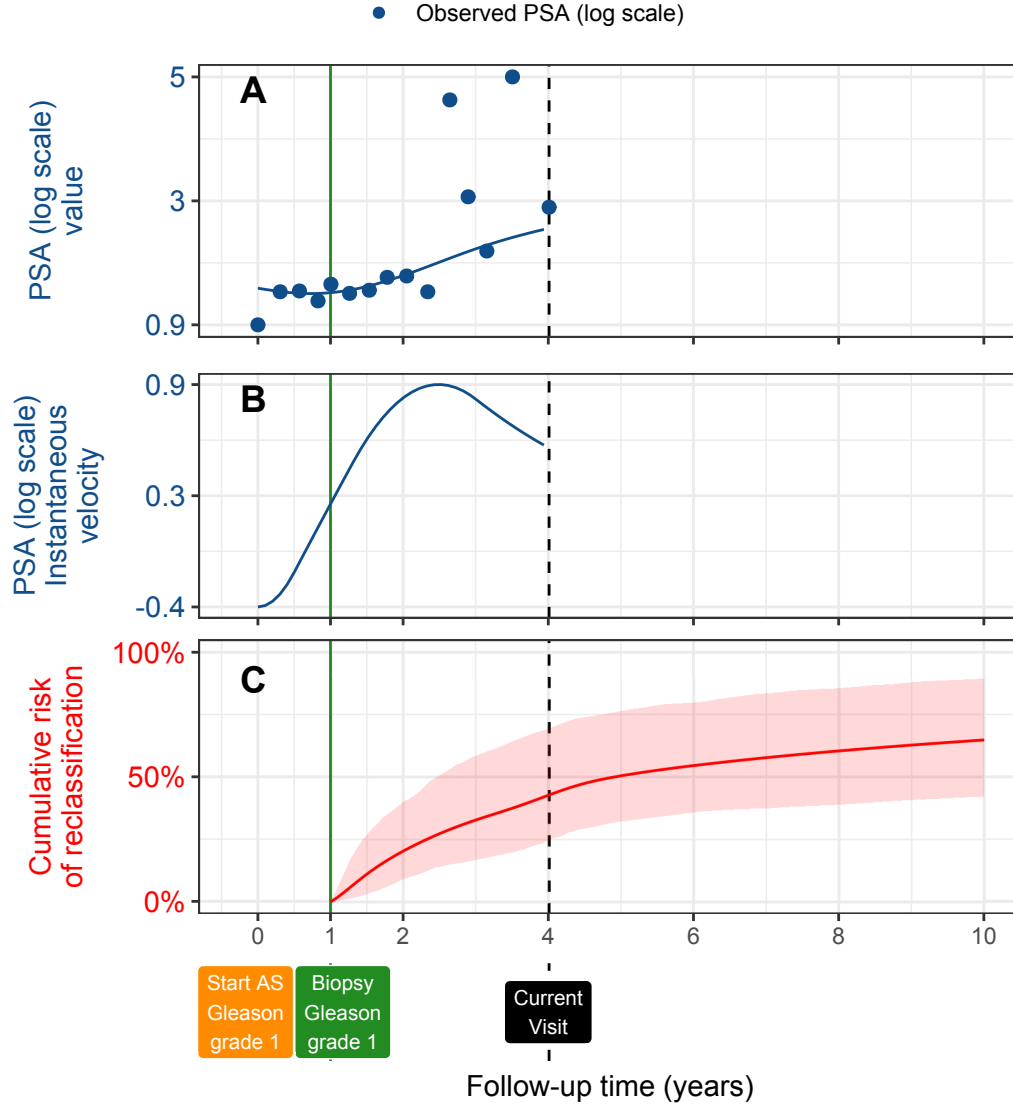


Figure 1: **Illustration of the joint model on a real PRIAS dataset patient.** **Panel A:** Observed (blue dots) and fitted PSA (solid blue line) measurements, log-transformed. **Panel B:** Estimated instantaneous velocity of PSA (log-transformed). **Panel C:** Predicted cumulative-risk of reclassification (95% credible interval shaded). Reclassification is defined as increase in Gleason grade [1] from grade 1 to 2 or higher. This risk of reclassification is available starting from the time of the latest negative biopsy (vertical green line at year 1 of follow-up). Joint model estimated it by combining the fitted PSA value and velocity (both on log scale of PSA) and time of latest negative biopsy. Black dashed line at year 4 denotes time of current visit.

The corresponding parameters are  $\alpha_1$  and  $\alpha_2$ , respectively. Lastly,  $h_0(t)$  is the baseline hazard at time  $t$ , and is modeled flexibly using P-splines [5]. More specifically:

$$\log h_0(t) = \gamma_{h_0,0} + \sum_{q=1}^Q \gamma_{h_0,q} B_q(t, \mathbf{v}),$$

where  $B_q(t, \mathbf{v})$  denotes the  $q$ -th basis function of a B-spline with knots  $\mathbf{v} = v_1, \dots, v_Q$  and vector of spline coefficients  $\gamma_{h_0}$ . To avoid choosing the number and position of knots in the spline, a relatively high number of knots (e.g., 15 to 20) are chosen and the corresponding B-spline regression coefficients  $\gamma_{h_0}$  are penalized using a differences penalty [5].

We estimate the parameters of the joint model using Markov chain Monte Carlo (MCMC) methods under the Bayesian framework. Let  $\boldsymbol{\theta}$  denote the vector of all of the parameters of the joint model. The joint model postulates that given the random effects, the time of reclassification, and the PSA measurements taken over time are all mutually independent. Under this assumption the posterior distribution of the parameters is given by:

$$\begin{aligned} p(\boldsymbol{\theta}, \mathbf{b} \mid \mathcal{D}_n) &\propto \prod_{i=1}^n p(l_i, r_i, \mathbf{y}_i \mid \mathbf{b}_i, \boldsymbol{\theta}) p(\mathbf{b}_i \mid \boldsymbol{\theta}) p(\boldsymbol{\theta}) \\ &\propto \prod_{i=1}^n p(l_i, r_i \mid \mathbf{b}_i, \boldsymbol{\theta}) p(\mathbf{y}_i \mid \mathbf{b}_i, \boldsymbol{\theta}) p(\mathbf{b}_i \mid \boldsymbol{\theta}) p(\boldsymbol{\theta}), \\ p(\mathbf{b}_i \mid \boldsymbol{\theta}) &= \frac{1}{\sqrt{(2\pi)^q \det(\mathbf{D})}} \exp(\mathbf{b}_i^T \mathbf{D}^{-1} \mathbf{b}_i), \end{aligned}$$

where, the likelihood contribution of the PSA outcome, conditional on the random effects is:

$$p(\mathbf{y}_i \mid \mathbf{b}_i, \boldsymbol{\theta}) = \frac{1}{(\sqrt{2\pi}\sigma^2)^{n_i}} \exp\left(-\frac{\|\mathbf{y}_i - \mathbf{m}_i\|^2}{\sigma^2}\right),$$

The likelihood contribution of the time of reclassification outcome is given by:

$$p(l_i, r_i \mid \mathbf{b}_i, \boldsymbol{\theta}) = \exp\left\{-\int_0^{l_i} h_i(s) ds\right\} - \exp\left\{-\int_0^{r_i} h_i(s) ds\right\}. \quad (3)$$

30 The integral in (3) does not have a closed-form solution, and therefore we  
 31 use a 15-point Gauss-Kronrod quadrature rule to approximate it.

32 We use independent normal priors with zero mean and variance 100 for  
 33 the fixed effects  $\{\beta_0, \dots, \beta_5\}$ , and inverse Gamma prior with shape and rate  
 34 both equal to 0.01 for the parameter  $\sigma^2$ . For the variance-covariance matrix  
 35  $\mathbf{D}$  of the random effects we take inverse Wishart prior with an identity scale  
 36 matrix and degrees of freedom equal to 5 (number of random effects). For  
 37 the relative risk model's parameter  $\gamma$  and the association parameters  $\alpha_1, \alpha_2$ ,  
 38 we use independent normal priors with zero mean and variance 100.

#### 39 *Appendix A.1. Assumption of t-distributed (df=3) Error Terms*

40 With regards to the choice of the distribution for the error term  $\varepsilon$  for  
 41 the PSA measurements (see Equation 1), we attempted fitting multiple joint  
 42 models differing in error distribution, namely t-distribution with three, and  
 43 four degrees of freedom, and a normal distribution for the error term. How-  
 44 ever, the model assumption for the error term were best met by the model  
 45 with t-distribution having three degrees of freedom. The quantile-quantile  
 46 plot of subject-specific residuals for the corresponding model in Panel A of  
 47 Figure 2, shows that the assumption of t-distributed (df=3) errors is reason-  
 48 ably met by the fitted model.

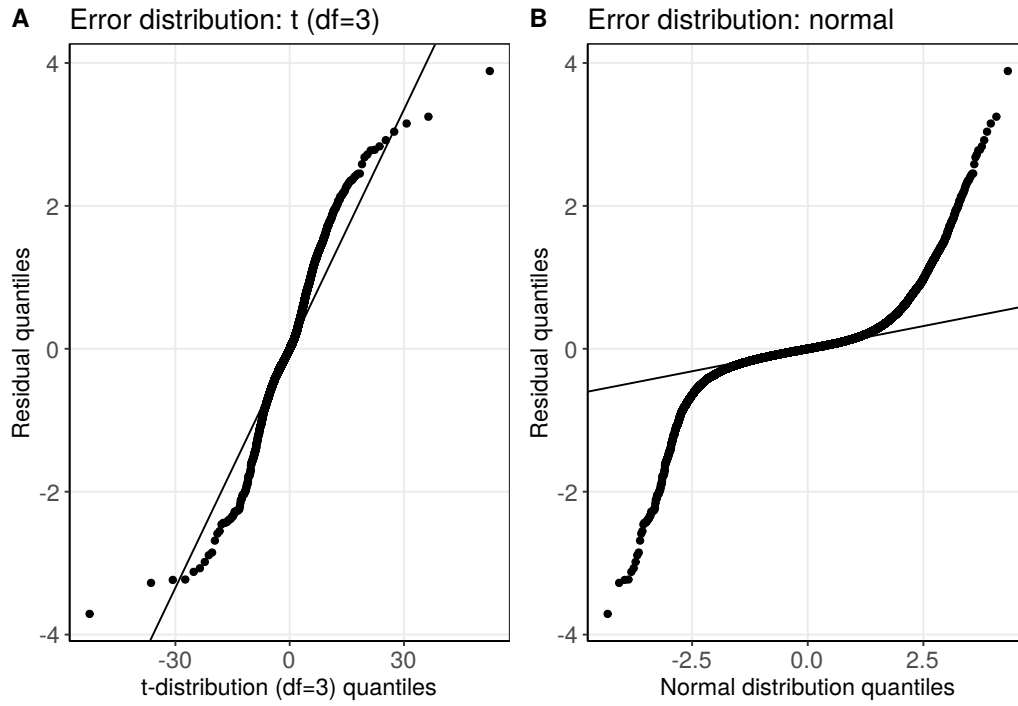


Figure 2: Quantile-quantile plot of subject-specific residuals from the joint models fitted to the PRIAS dataset. **Panel A:** model assuming a t-distribution ( $df=3$ ) for the error term  $\varepsilon$  (see Equation 1). **Panel B:** model assuming a normal distribution for the error term  $\varepsilon$ .

Table 1: Estimated variance-covariance matrix  $\mathbf{D}$  of the random effects  $\mathbf{b} = (b_0, b_1, b_2, b_3, b_4)$  from the joint model fitted to the PRIAS dataset. The variances of the random effects are highlighted along the diagonal of the variance-covariance matrix.

Random Effects	$b_0$	$b_1$	$b_2$	$b_3$	$b_4$
$b_0$	<b>0.229</b>	0.030	0.023	0.073	0.007
$b_1$	0.030	<b>0.149</b>	0.098	0.171	0.085
$b_2$	0.023	0.098	<b>0.276</b>	0.335	0.236
$b_3$	0.073	0.171	0.335	<b>0.560</b>	0.359
$b_4$	0.007	0.085	0.236	0.359	<b>0.351</b>

Table 2: Estimated mean and 95% credible interval for the parameters of the longitudinal sub-model (see Equation 1) for the PSA outcome.

Variable	Mean	Std. Dev	2.5%	97.5%	P
Intercept	2.129	0.060	2.009	2.244	<0.001
Age	0.008	0.001	0.007	0.010	<0.001
Spline: [0.0, 0.5] years	0.063	0.007	0.051	0.075	<0.001
Spline: [0.5, 1.3] years	0.196	0.010	0.177	0.217	<0.001
Spline: [1.3, 3.0] years	0.244	0.014	0.217	0.272	<0.001
Spline: [3.0, 6.3] years	0.382	0.014	0.356	0.410	<0.001
$\sigma$	0.139	0.001	0.138	0.140	

## 49 Appendix A.2. Results

50 The joint model was fitted using the R package **JMbayes** [8]. This pack-  
 51 age utilizes the Bayesian methodology to estimate model parameters. The  
 52 corresponding posterior parameter estimates are shown in Table 2 (longitu-  
 53 dinal sub-model for PSA outcome) and Table 3 (relative risk sub-model).  
 54 The parameter estimates for the variance-covariance matrix  $\mathbf{D}$  from the lon-  
 55 gitudinal sub-model for PSA are shown in the following Table 1:

56 For the PSA mixed effects sub-model parameter estimates (see Equa-  
 57 tion 1), in Table 2 we can see that the age of the patient trivially affects  
 58 the baseline  $\log_2(\text{PSA} + 1)$  measurement. Since the longitudinal evolution of  
 59  $\log_2(\text{PSA} + 1)$  measurements is modeled with non-linear terms, the interpre-  
 60 tation of the coefficients corresponding to time is not straightforward. In lieu  
 61 of the interpretation, in Figure 4 we present plots of observed versus fitted  
 62 PSA profiles for nine randomly selected patients.

63 For the relative risk sub-model (see Equation 2), the parameter estimates  
 64 in Table 3 show that  $\log_2(\text{PSA} + 1)$  velocity and age of the patient were

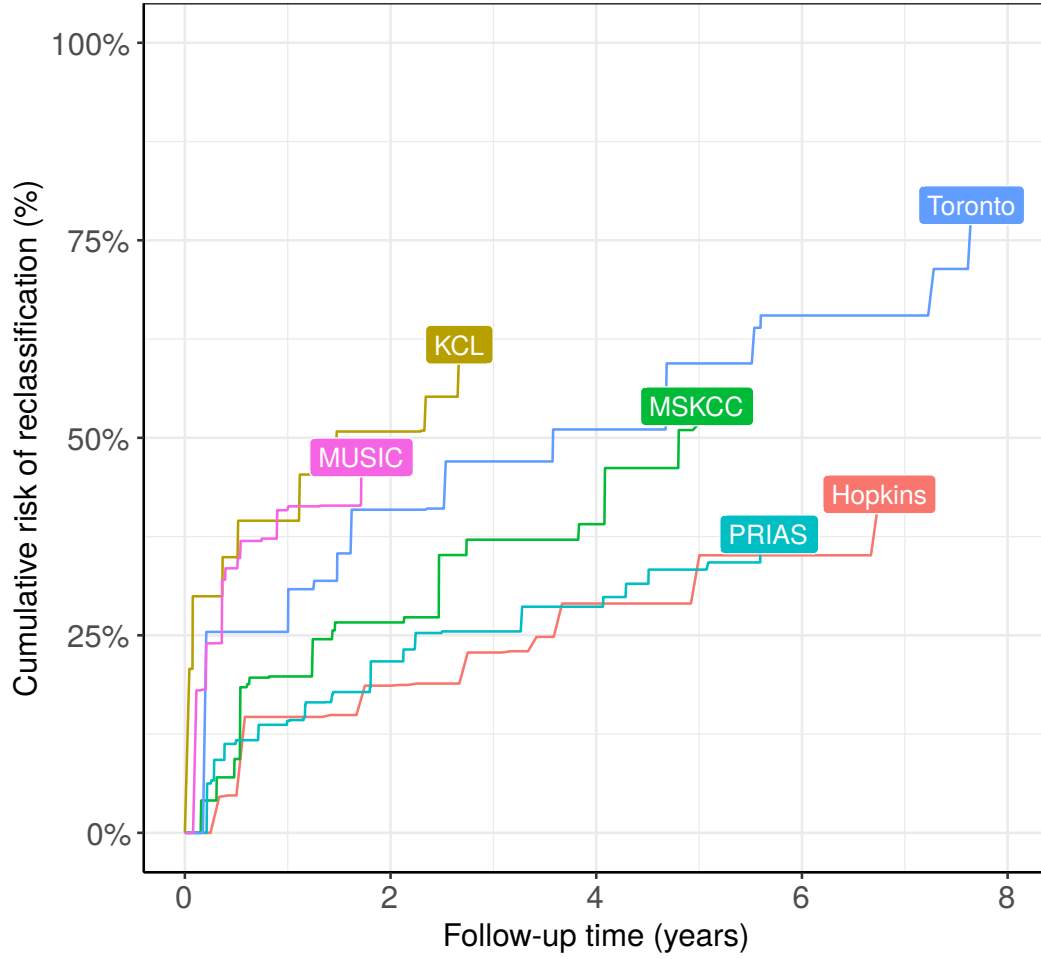


Figure 3: **Nonparametric estimate [6] of cumulative risk of reclassification** in the world's largest AS cohort PRIAS, and largest five AS cohorts from the GAP3 database [7]. Abbreviations are *Hopkins*: Johns Hopkins Active Surveillance, *PRIAS*: Prostate Cancer International Active Surveillance, *Toronto*: University of Toronto Active Surveillance, *MSKCC*: Memorial Sloan Kettering Cancer Center Active Surveillance, *KCL*: King's College London Active Surveillance, *MUSIC*: Michigan Urological Surgery Improvement Collaborative AS.



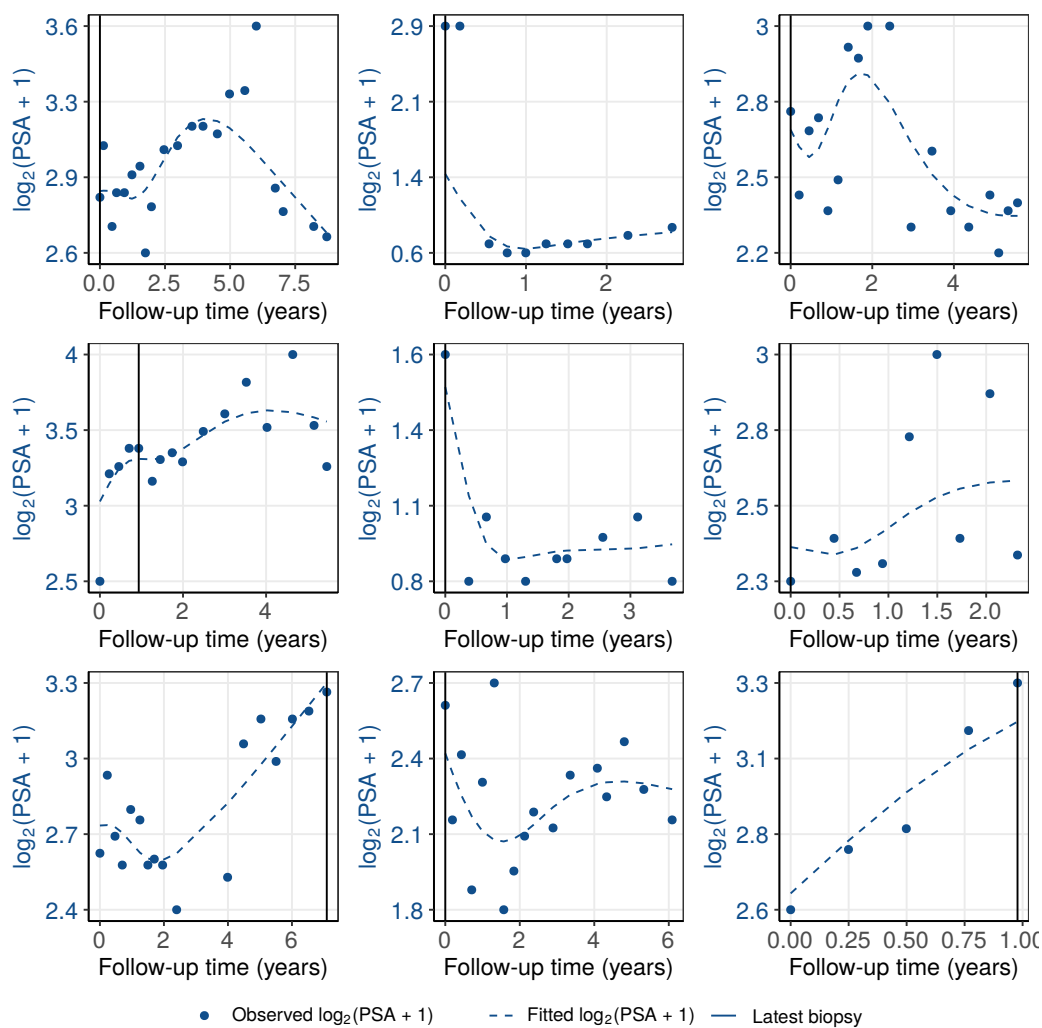


Figure 4: Fitted versus observed  $\log_2(\text{PSA} + 1)$  profiles for nine randomly selected PRIAS patients. The fitted profiles utilize information from the observed PSA measurements, and time of the latest biopsy.

Table 3: Estimated mean and 95% credible interval for the parameters of the relative risk sub-model (see Equation 2) of the joint model fitted to the PRIAS dataset.

Variable	Mean	Std. Dev	2.5%	97.5%	P
Age	0.037	0.006	0.025	0.049	<0.001
Fitted $\log_2(\text{PSA} + 1)$ value	-0.012	0.076	-0.164	0.135	0.856
Fitted $\log_2(\text{PSA} + 1)$ velocity	2.266	0.299	1.613	2.767	<0.001

Table 4: Hazard (of reclassification) ratio and 95% credible interval (CI), for an increase in the variables of relative risk sub-model, from their 25-th percentile ( $P_{25}$ ) to their 75-th percentile ( $P_{75}$ ). Except for age, quartiles for all other variables are based on their fitted values obtained from the joint model fitted to the PRIAS dataset.

Variable	$P_{25}$	$P_{75}$	Hazard ratio [95% CI]
Age	61	71	1.455 [1.285, 1.631]
Fitted $\log_2(\text{PSA} + 1)$ value	2.360	3.078	0.991 [0.889, 1.102]
Fitted $\log_2(\text{PSA} + 1)$ velocity	-0.085	0.308	2.433 [1.883, 2.962]

significantly associated with the hazard of reclassification.

It is important to note that since age, and  $\log_2(\text{PSA} + 1)$  value and velocity are all measured on different scales, a comparison between the corresponding parameter estimates is not easy. To this end, in Table 4, we present the hazard ratio of reclassification, for an increase in the aforementioned variables from their 25-th to the 75-th percentile. For example, an increase in fitted  $\log_2(\text{PSA} + 1)$  velocity from -0.085 to 0.308 (fitted 25-th and 75-th percentiles) corresponds to a hazard ratio of 2.433. The interpretation for the rest is similar.

## 74 Appendix B. Risk Predictions for Reclassification

Let us assume a new patient  $j$ , for whom we need to estimate the risk of reclassification. Let his current follow-up visit time be  $s$ , latest time of biopsy be  $t$ , observed vector PSA measurements be  $\mathcal{Y}_j(s)$ . The combined information from the observed data about the time of reclassification, is given by the following posterior predictive distribution  $g(T_j^*)$  of his time  $T_j^*$  of reclassification:

$$\begin{aligned} g(T_j^*) &= p\{T_j^* \mid T_j^* > t, \mathcal{Y}_j(s), \mathcal{D}_n\} \\ &= \int \int p(T_j^* \mid T_j^* > t, \mathbf{b}_j, \boldsymbol{\theta}) \\ &\quad \times p\{\mathbf{b}_j \mid T_j^* > t, \mathcal{Y}_j(s), \boldsymbol{\theta}\} p(\boldsymbol{\theta} \mid \mathcal{D}_n) d\mathbf{b}_j d\boldsymbol{\theta}. \end{aligned}$$

75 The distribution  $g(T_j^*)$  depends not only depends on the observed data of the  
 76 patient  $T_j^* > t, \mathcal{Y}_j(s)$ , but also depends on the information from the PRIAS  
 77 dataset  $\mathcal{D}_n$ . To this the the posterior distribution of random effects  $\mathbf{b}_j$  and  
 78 posterior distribution of the vector of all parameters  $\boldsymbol{\theta}$  are utilized, respec-  
 79 tively. The distribution  $g(T_j^*)$  can be estimated as detailed in Rizopoulos  
 80 et al. [9]. Since, majority of the prostate cancer patients may not obtain  
 81 reclassification in the current follow-up period of PRIAS (thirteen years),  
 82  $g(T_j^*)$  can only be estimated for time points falling within the thirteen year  
 83 follow-up.

The cumulative risk of reclassification can be derived from  $g(T_j^*)$  as given in [9]. It is given by:

$$R_j(u \mid t, s) = \Pr\{T_j^* > u \mid T_j^* > t, \mathcal{Y}_j(s), \mathcal{D}_n\}, \quad u \geq t. \quad (4)$$

84 The personalized risk profile of the patient (see Panel C, Figure 5) updates  
 85 as more data is gathered over follow-up visits.

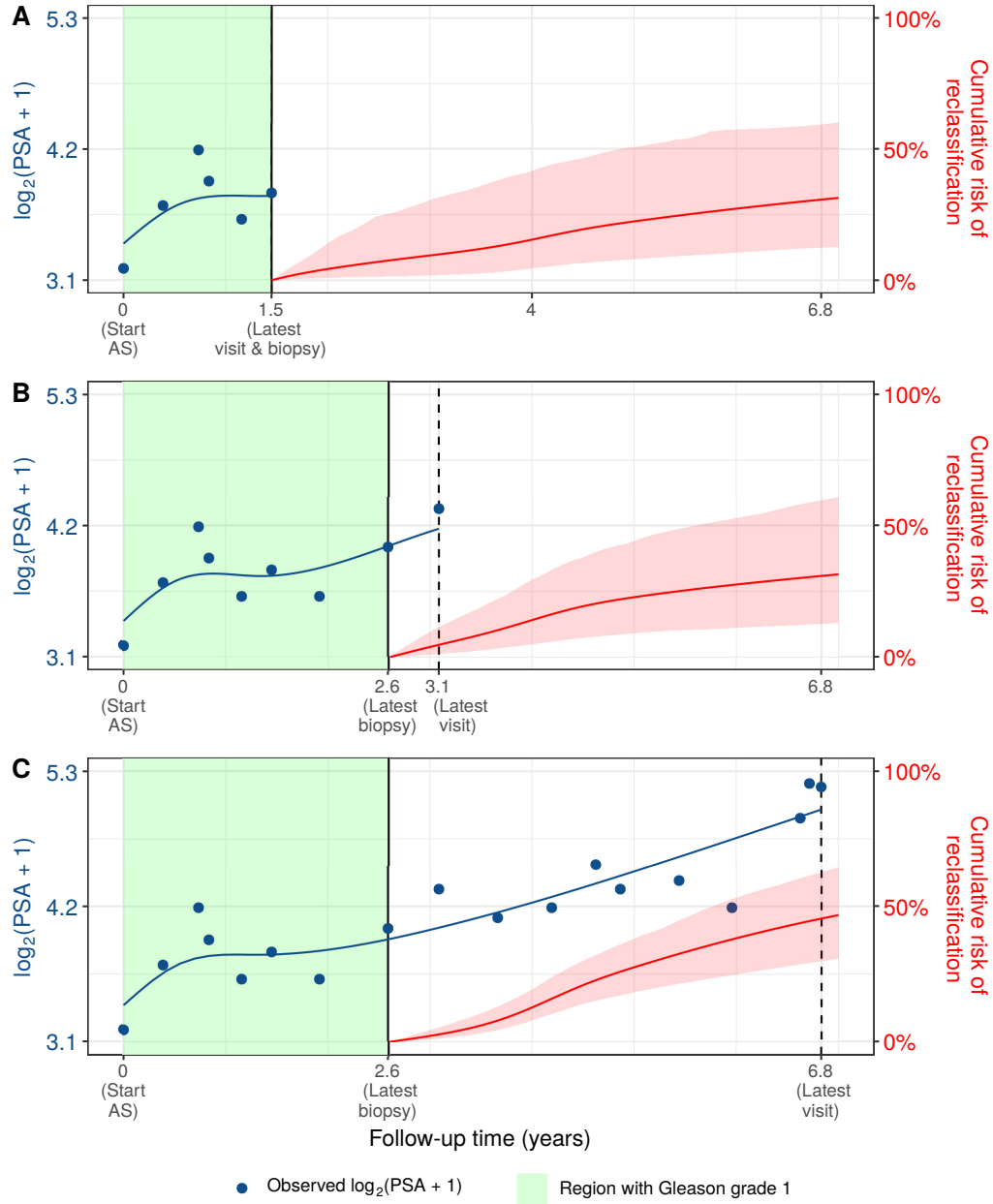


Figure 5: **Cumulative risk of (reclassification) changing dynamically over follow-up** as more patient data is gathered. The three **Panels A,B and C:** are ordered by the time of the latest visit (dashed vertical black line) of a new patient. At each of the latest follow-up visits, we combine the accumulated PSA measurements (shown in blue), and latest time of negative biopsy (solid vertical black line) to obtain the updated cumulative risk profile (shown in red) of the patient.

## 86 *Appendix B.1. Validation of Risk Predictions*

87 We wanted to check the discrimination and calibration of our model.  
88 At the same time we also wanted to check if our model could be used in  
89 other cohorts. To this end, we validated the predictions of reclassification  
90 internally within the PRIAS dataset, as well as externally in largest five AS  
91 cohorts from the GAP3 database [7]. These are the University of Toronto  
92 AS (Toronto), Johns Hopkins AS (Hopkins), Memorial Sloan Kettering Can-  
93 cer Center AS (MSKCC), King’s College London AS (KCL), and Michigan  
94 Urological Surgery Improvement Collaborative AS (MUSIC). In all of these  
95 cohorts, we calculated the area under the receiver operating characteristic  
96 curve or AUC [9] as a measure of discrimination between patients who obtain  
97 reclassification and those do not obtain reclassification. We also calculated  
98 root mean squared prediction error or RMSPE [9] as a measure of calibra-  
99 tion. Both AUC and RMSPE take a value between 0 and 1. Ideally RMSPE  
100 should be 0 and AUC should 1. In addition, it is preferred that  $\text{AUC} >$   
101  $0.5$  because an  $\text{AUC} \leq 0.5$  indicates that the model performs worse than  
102 random discrimination. Since AS studies are longitudinal in nature, AUC  
103 and RMSPE are also time dependent. More specifically, given the time of  
104 latest biopsy  $t$ , and history of PSA measurements up to time  $s$ , we calculate  
105 AUC and RMSPE for a medically relevant time frame  $(t, s]$ , within which  
106 the occurrence of reclassification is of interest. In the case of prostate cancer,  
107 at any point in time  $s$  it is of interest to identify patients who may have ob-  
108 tained reclassification in the last one year  $(s - 1, s]$ . That is we set  $t = s - 1$ .  
109 We then calculate AUC and RMSPE at a gap of every six months (follow-up  
110 schedule of PRIAS) until year five (95-percentile of the observed times of  
111 reclassification), that is,  $s \in \{1, 1.5, \dots, 5\}$  years. The resulting estimates are  
112 summarized in Figure 6, and in Table 5 to Table 10.

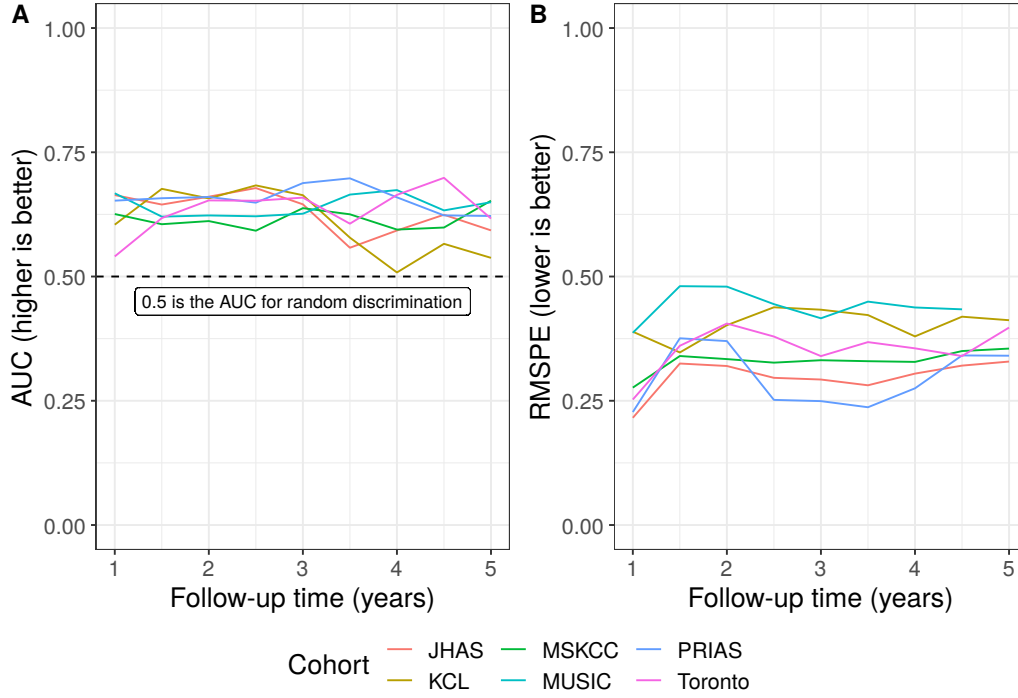


Figure 6: **Validation of predictions of Gleason  $\geq 7$  (reclassification).** In **Panel A** we can see that the time dependent area under the receiver operating characteristic curve or AUC (measure of discrimination) is above 0.5 in PRIAS (internal validation), and in Toronto, JHAS, MSKCC, KCL, and MUSIC AS cohorts (external validation). In **Panel B** we can see that the time dependent root mean squared prediction error or RMSPE (measure of calibration) is similar for PRIAS, and JHAS and Toronto cohorts. The bootstrapped 95% confidence interval for these estimates are presented in Table 5 to Table 9. Full names of Cohorts are *PRIAS*: Prostate Cancer International Active Surveillance, *Toronto*: University of Toronto Active Surveillance, *JHAS*: Johns Hopkins Active Surveillance, *MSKCC*: Memorial Sloan Kettering Cancer Center Active Surveillance, *KCL*: King's College London Active Surveillance, *MUSIC*: Michigan Urological Surgery Improvement Collaborative Active Surveillance.

Table 5: **Internal Validation of predictions of Gleason  $\geq 7$  (reclassification) in PRIAS cohort.** The area under the receiver operating characteristic curve or AUC (measure of discrimination) root mean squared prediction error or RMSPE (measure of calibration) are calculated over the follow-up period at a gap of 6 months. In addition bootstrapped 95% confidence intervals (CI) are also presented.

Follow-up period (years)	AUC (95% CI)	RMSPE (95%CI)
0.0 to 1.0	0.656 [0.623, 0.690]	0.227 [0.223, 0.236]
0.5 to 1.5	0.657 [0.641, 0.671]	0.376 [0.371, 0.382]
1.0 to 2.0	0.663 [0.651, 0.678]	0.371 [0.364, 0.379]
1.5 to 2.5	0.650 [0.600, 0.684]	0.253 [0.245, 0.263]
2.0 to 3.0	0.676 [0.641, 0.725]	0.252 [0.241, 0.262]
2.5 to 3.5	0.689 [0.629, 0.732]	0.238 [0.224, 0.251]
3.0 to 4.0	0.652 [0.614, 0.709]	0.273 [0.263, 0.285]
3.5 to 4.5	0.625 [0.591, 0.663]	0.338 [0.326, 0.349]
4.0 to 5.0	0.623 [0.587, 0.657]	0.338 [0.325, 0.350]

Table 6: **External Validation of predictions of Gleason  $\geq 7$  (reclassification) in University of Toronto Active Surveillance cohort.** The area under the receiver operating characteristic curve or AUC (measure of discrimination) root mean squared prediction error or RMSPE (measure of calibration) are calculated over the follow-up period at a gap of 6 months. In addition bootstrapped 95% confidence intervals (CI) are also presented.

Follow-up period (years)	AUC (95% CI)	RMSPE (95%CI)
0.0 to 1.0	0.540 [0.493, 0.595]	0.252 [0.236, 0.272]
0.5 to 1.5	0.618 [0.562, 0.660]	0.361 [0.350, 0.373]
1.0 to 2.0	0.653 [0.580, 0.719]	0.405 [0.384, 0.428]
1.5 to 2.5	0.652 [0.596, 0.727]	0.379 [0.358, 0.408]
2.0 to 3.0	0.659 [0.565, 0.743]	0.340 [0.303, 0.369]
2.5 to 3.5	0.606 [0.548, 0.676]	0.368 [0.340, 0.401]
3.0 to 4.0	0.664 [0.583, 0.736]	0.355 [0.324, 0.391]
3.5 to 4.5	0.699 [0.610, 0.773]	0.340 [0.310, 0.374]
4.0 to 5.0	0.617 [0.546, 0.705]	0.397 [0.355, 0.425]

Table 7: **External Validation of predictions of Gleason  $\geq 7$  (reclassification) in Johns Hopkins Active Surveillance cohort.** The area under the receiver operating characteristic curve or AUC (measure of discrimination) root mean squared prediction error or RMSPE (measure of calibration) are calculated over the follow-up period at a gap of 6 months. In addition bootstrapped 95% confidence intervals (CI) are also presented.

Follow-up period (years)	AUC (95% CI)	RMSPE (95%CI)
0.0 to 1.0	0.664 [0.604, 0.743]	0.216 [0.198, 0.236]
0.5 to 1.5	0.645 [0.597, 0.695]	0.325 [0.310, 0.339]
1.0 to 2.0	0.661 [0.615, 0.707]	0.320 [0.300, 0.335]
1.5 to 2.5	0.678 [0.587, 0.736]	0.296 [0.277, 0.312]
2.0 to 3.0	0.645 [0.595, 0.701]	0.293 [0.268, 0.317]
2.5 to 3.5	0.558 [0.445, 0.622]	0.281 [0.256, 0.307]
3.0 to 4.0	0.593 [0.498, 0.693]	0.305 [0.281, 0.329]
3.5 to 4.5	0.624 [0.527, 0.690]	0.321 [0.294, 0.340]
4.0 to 5.0	0.593 [0.483, 0.694]	0.329 [0.306, 0.352]

Table 8: **External Validation of predictions of Gleason  $\geq 7$  (reclassification) in Memorial Sloan Kettering Cancer Center Active Surveillance cohort.** The area under the receiver operating characteristic curve or AUC (measure of discrimination) root mean squared prediction error or RMSPE (measure of calibration) are calculated over the follow-up period at a gap of 6 months. In addition bootstrapped 95% confidence intervals (CI) are also presented.

Follow-up period (years)	AUC (95% CI)	RMSPE (95%CI)
0.0 to 1.0	0.626 [0.558, 0.681]	0.276 [0.260, 0.297]
0.5 to 1.5	0.605 [0.539, 0.666]	0.340 [0.321, 0.360]
1.0 to 2.0	0.612 [0.564, 0.672]	0.334 [0.316, 0.350]
1.5 to 2.5	0.592 [0.502, 0.670]	0.327 [0.306, 0.345]
2.0 to 3.0	0.638 [0.548, 0.720]	0.332 [0.304, 0.363]
2.5 to 3.5	0.625 [0.542, 0.717]	0.330 [0.303, 0.371]
3.0 to 4.0	0.594 [0.511, 0.655]	0.328 [0.281, 0.368]
3.5 to 4.5	0.599 [0.481, 0.740]	0.350 [0.312, 0.373]
4.0 to 5.0	0.653 [0.562, 0.724]	0.355 [0.320, 0.380]



Table 9: **External Validation of predictions of Gleason  $\geq 7$  (reclassification) in King’s College London Active Surveillance cohort.** The area under the receiver operating characteristic curve or AUC (measure of discrimination) root mean squared prediction error or RMSPE (measure of calibration) are calculated over the follow-up period at a gap of 6 months. In addition bootstrapped 95% confidence intervals (CI) are also presented.

Follow-up period (years)	AUC (95% CI)	RMSPE (95%CI)
0.0 to 1.0	0.604 [0.548, 0.663]	0.389 [0.366, 0.411]
0.5 to 1.5	0.676 [0.603, 0.744]	0.347 [0.328, 0.372]
1.0 to 2.0	0.657 [0.578, 0.728]	0.402 [0.368, 0.426]
1.5 to 2.5	0.683 [0.595, 0.773]	0.438 [0.395, 0.469]
2.0 to 3.0	0.664 [0.576, 0.735]	0.433 [0.396, 0.467]
2.5 to 3.5	0.578 [0.443, 0.712]	0.422 [0.345, 0.479]
3.0 to 4.0	0.508 [0.358, 0.670]	0.380 [0.313, 0.452]
3.5 to 4.5	0.566 [0.346, 0.776]	0.419 [0.354, 0.484]
4.0 to 5.0	0.538 [0.295, 0.759]	0.412 [0.345, 0.470]

Table 10: **External Validation of predictions of Gleason  $\geq 7$  (reclassification) in Michigan Urological Surgery Improvement Collaborative Active Surveillance cohort.** The area under the receiver operating characteristic curve or AUC (measure of discrimination) root mean squared prediction error or RMSPE (measure of calibration) are calculated over the follow-up period at a gap of 6 months. In addition bootstrapped 95% confidence intervals (CI) are also presented.

Follow-up period (years)	AUC (95% CI)	RMSPE (95%CI)
0.0 to 1.0	0.667 [0.616, 0.703]	0.387 [0.369, 0.409]
0.5 to 1.5	0.620 [0.566, 0.646]	0.481 [0.462, 0.495]
1.0 to 2.0	0.623 [0.569, 0.666]	0.480 [0.459, 0.501]
1.5 to 2.5	0.621 [0.580, 0.677]	0.444 [0.418, 0.472]
2.0 to 3.0	0.626 [0.464, 0.710]	0.416 [0.376, 0.459]
2.5 to 3.5	0.665 [0.554, 0.796]	0.449 [0.390, 0.493]
3.0 to 4.0	0.674 [0.540, 0.757]	0.438 [0.374, 0.483]
3.5 to 4.5	0.633 [0.410, 0.865]	0.434 [0.346, 0.485]
4.0 to 5.0	0.650 [0.248, 0.946]	– [–, –]

### 113 Appendix C. Personalized Biopsies Based on Risk of GS7

114 Consider some real patients from the PRIAS database shown in Figure 7  
 115 to Figure 10. We intend to develop personalized schedule of biopsies for  
 116 these patients. Using the joint model fitted to the PRIAS dataset, we first  
 117 obtain their cumulative risk of GS7 over the entire follow-up period (see  
 118 Equation 4). This cumulative risk accounts for their entire history of PSA  
 119 as well as the time of their latest negative biopsy. For a new patient  $j$  we  
 120 suggest a personalized risk based biopsy at time  $s$  if their cumulative risk of  
 121 GS7 denoted by  $R_j(s | t, s)$  at  $s$ , given the time of their latest negative biopsy  
 122  $t$ , is above a certain threshold (e.g., 10% risk). Suppose that in this way a  
 123 decision of biopsy is taken at time  $s$ . Since patients may be removed from  
 124 AS upon detection of GS7, schedule of future biopsies is made by assuming  
 125 that GS7 is not detected at time  $s$ . Thus, for a decision of biopsy at the next  
 126 visit time  $s + 1$ , the cumulative risk of GS7 denoted by  $R_j(s + 1 | s, s)$  that  
 127 the time of latest negative biopsy is  $s$ . Similarly, if  $R_j(s + 1 | s, s) < 10\%$ ,  
 128 then we decide for a biopsy at a subsequent time  $s + 2$  using the threshold  
 129  $R_j(s + 2 | s, s)$ . On the other hand if  $R_j(s + 1 | s, s) \geq 10\%$  then then we  
 130 decide for a biopsy at time  $s + 2$  using the threshold  $R_j(s + 2 | s + 1, s)$ .  
 131 While scheduling these biopsies we always maintain a minimum gap of one  
 132 year. Personalized schedules can also be made with any other risk threshold  
 133 such as 5% or 15%.

To assist patients in making an informed choice for a schedule, be it personalized or fixed, we provide them patient-specific consequences of following each schedule. To this end, we first calculate the probability of occurrence of GS7 between successive biopsies of each schedule. Using these probabilities we then obtain the expected delay in detection of GS7 for following that schedule. Thus, patients have a method to compare across various schedules in terms of the personalized burden (time and total biopsies), and personalized benefit (less delay in detection of GS7 is beneficial). Suppose once again that for patient  $j$ , the time of latest negative biopsy is  $t$ , and current visit time is  $s > t$ . Then equation for the expected delay  $D_j(\mathcal{S} | t, s)$  in detection of GS7 using schedule of biopsies  $\mathcal{S} = \{t_1, \dots, t_h\}$ , where  $t_1 \geq s$ , and  $t_h$  is

the horizon time up to which we want to schedule biopsies, is given by:

$$D_j(\mathcal{S} \mid t, s) = \sum_{v=1}^{h-1} \left\{ R_j(t_{v+1} \mid t, s) - R_j(t_v \mid t, s) \right\} \times \left\{ t_{v+1} - t_v - \int_{t_v}^{t_{v+1}} \frac{R_j(t_{v+1} \mid t, s) - R_j(u \mid t, s)}{R_j(t_{v+1} \mid t, s) - R_j(t_v \mid t, s)} du \right\} \quad (5)$$

134 The personalized and fixed schedules, and their consequences for a few real  
 135 patients from the PRIAS dataset are shown in Figure 7 to Figure 10. We  
 136 maintained a minimum gap of one year between biopsies as advised by the  
 137 PRIAS protocol. In addition, we scheduled biopsies only for the first ten years  
 138 follow-up because of limited follow-up data period of PRIAS. A compulsory  
 139 biopsy was done at year ten of follow-up in all schedules for meaningful  
 140 comparison of their expected delays in detection of GS7.

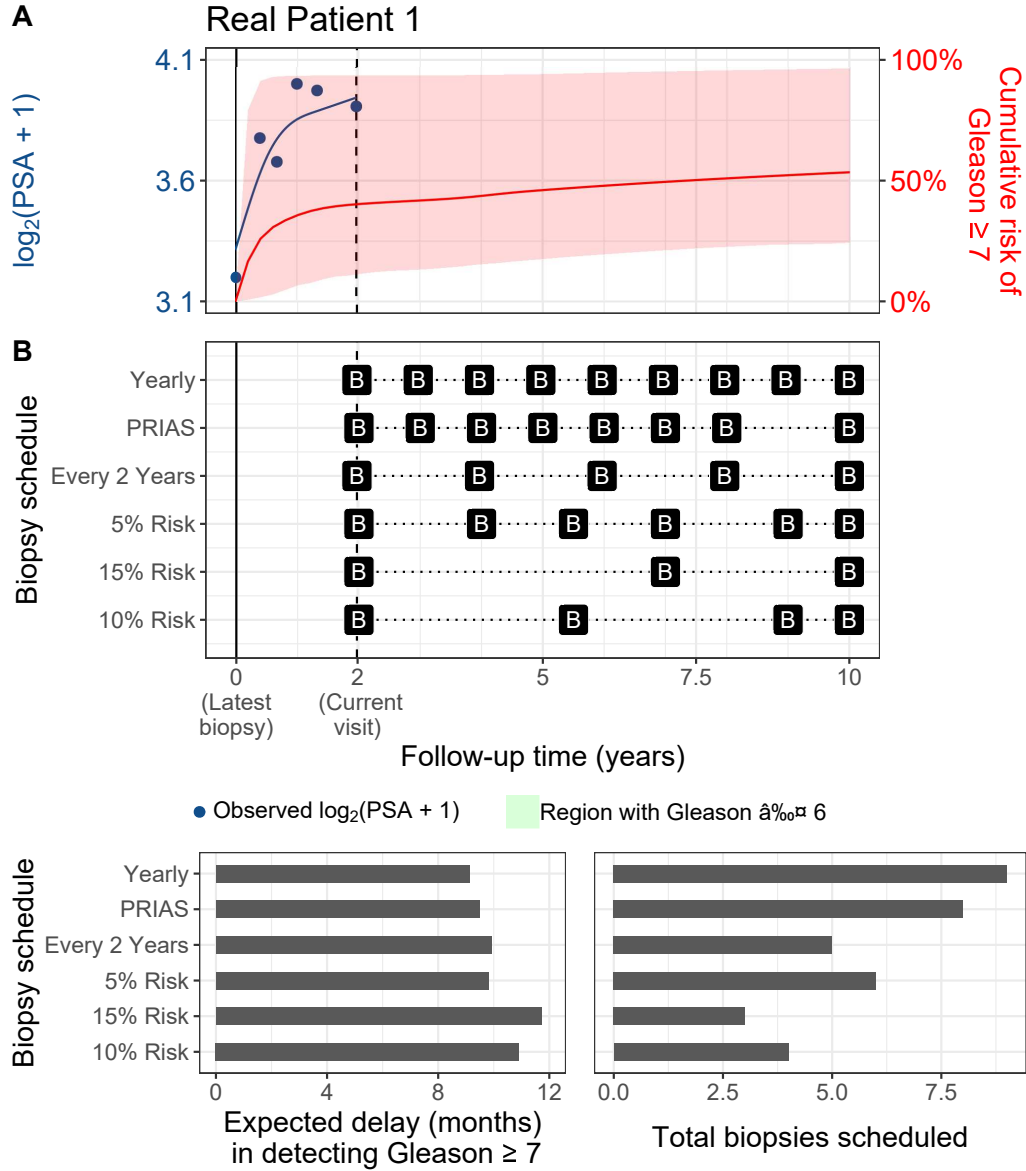


Figure 7: **Personalized and fixed schedules of biopsies for patient 1.** **Panel A:** shows the observed and fitted  $\log_2(\text{PSA} + 1)$  measurements (Equation 1), and the dynamic cumulative risk of Gleason  $\geq 7$  (see Appendix B) over follow-up period. **Panel B** shows the personalized and fixed schedules of biopsies with a 'B' indicating times of biopsies. In the bottom two panels, the various schedules are compared in terms of the number of biopsies they schedule, and the expected delay in detection of Gleason  $\geq 7$  if they are followed.

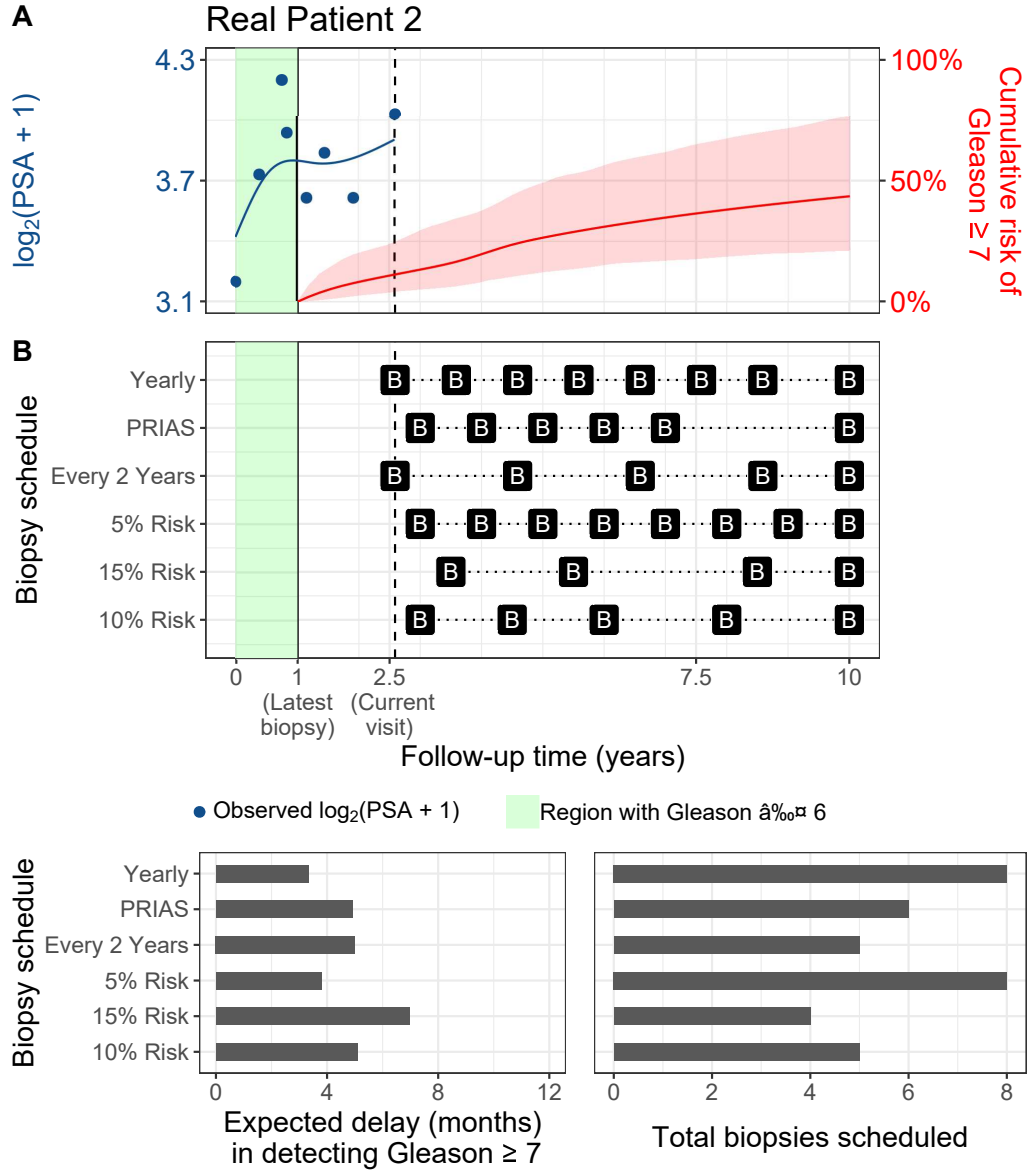


Figure 8: **Personalized and fixed schedules of biopsies for patient 2.** **Panel A:** shows the observed and fitted  $\log_2(\text{PSA} + 1)$  measurements (Equation 1), and the dynamic cumulative risk of Gleason  $\geq 7$  (see Appendix B) over follow-up period. **Panel B** shows the personalized and fixed schedules of biopsies with a 'B' indicating times of biopsies. In the bottom two panels, the various schedules are compared in terms of the number of biopsies they schedule, and the expected delay in detection of Gleason  $\geq 7$  if they are followed.

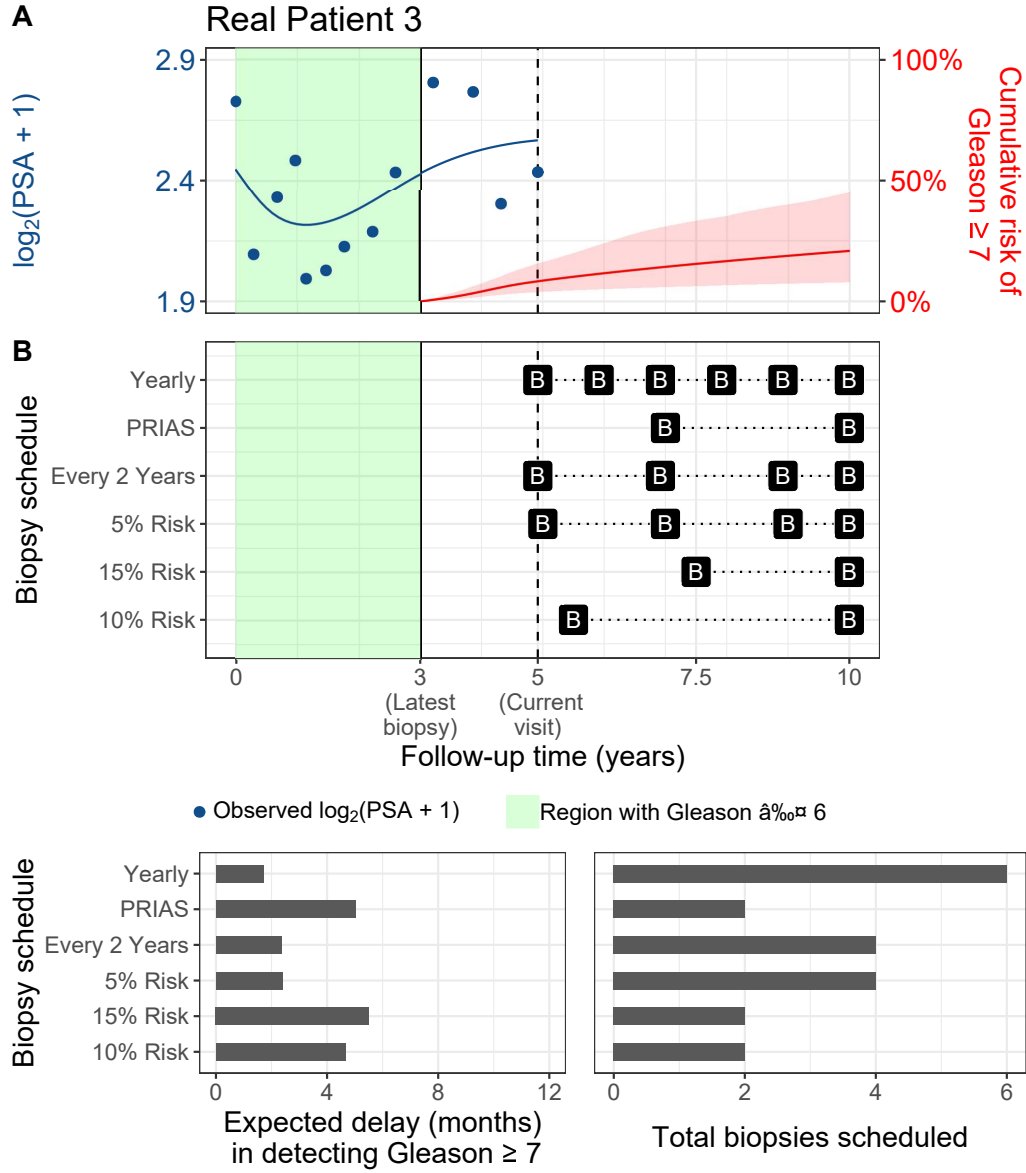


Figure 9: **Personalized and fixed schedules of biopsies for patient 3.** **Panel A:** shows the observed and fitted  $\log_2(\text{PSA} + 1)$  measurements (Equation 1), and the dynamic cumulative risk of Gleason  $\geq 7$  (see Appendix B) over follow-up period. **Panel B** shows the personalized and fixed schedules of biopsies with a ‘B’ indicating times of biopsies. In the bottom two panels, the various schedules are compared in terms of the number of biopsies they schedule, and the expected delay in detection of Gleason  $\geq 7$  if they are followed.

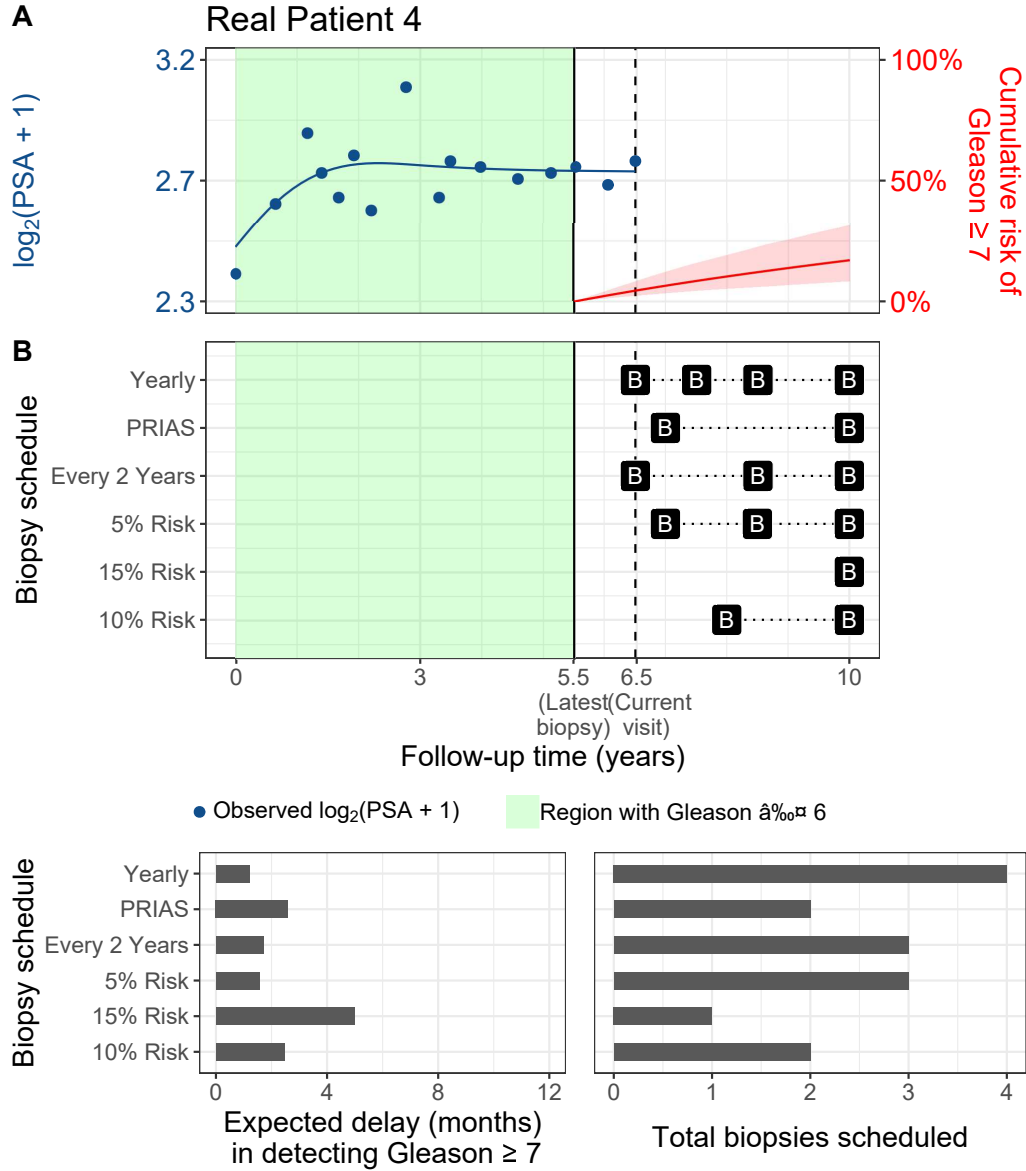


Figure 10: **Personalized and fixed schedules of biopsies for patient 4.** **Panel A:** shows the observed and fitted  $\log_2(\text{PSA} + 1)$  measurements (Equation 1), and the dynamic cumulative risk of Gleason  $\geq 7$  (see Appendix B) over follow-up period. **Panel B** shows the personalized and fixed schedules of biopsies with a 'B' indicating times of biopsies. In the bottom two panels, the various schedules are compared in terms of the number of biopsies they schedule, and the expected delay in detection of Gleason  $\geq 7$  if they are followed.

## Appendix D. Web Application for Practical Use of Personalized Schedule of Biopsies

We implemented our methodology in a web-application to assist patients and doctors in better decision making. It works on desktop as well as mobile devices. It is hosted at [https://emcbiostatistics.shinyapps.io/prias\\_biopsy\\_recommender/](https://emcbiostatistics.shinyapps.io/prias_biopsy_recommender/).

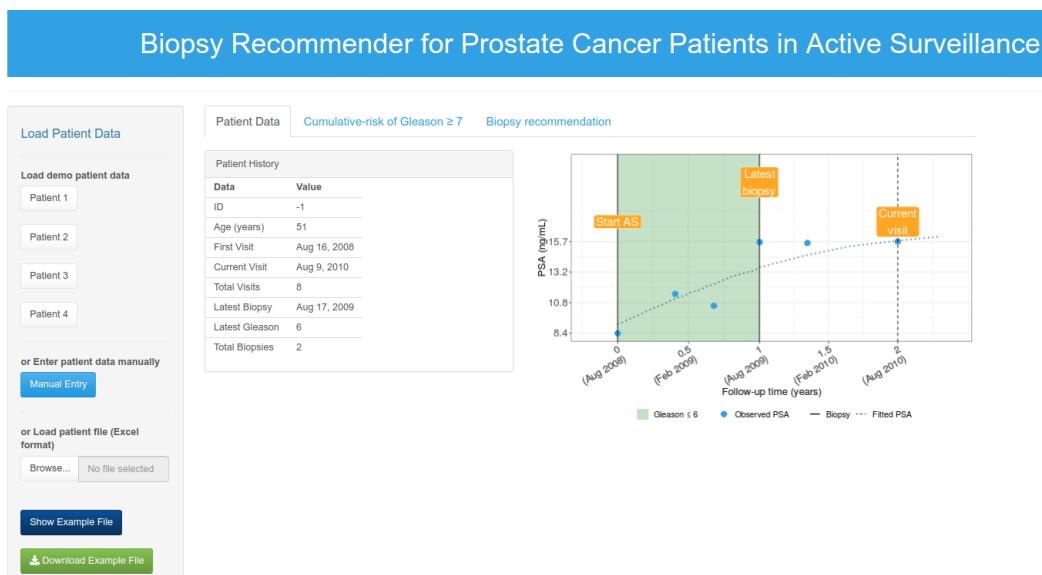


Figure 11: Landing page of the web-application. Panel on the left allows users to load patient data and panel on the right provides information. Patient data can be entered manually, or via Excel files. In addition, demo patient data is already uploaded to assist users in understanding the web-application.



**Patient Data Manual Entry Form**

Enter patient age (years)

60

Enter date of low-grade prostate cancer diagnosis

31-12-2018

Enter time (years) of previous biopsies with Gleason  $\leq 6$ . Count years since diagnosis, and separate them by comma.

0, 1, 2, 5

Enter time (years) of all follow-up visits on which PSA was measured. Count years since diagnosis, and separate them by comma.

0, 0.5, 1, 1.5, 2, 2.5, 3, 3.5

Enter PSA values (ng/mL). Separate them by comma.

5.7, 3.2, 12, 8.5, 15, 21.7, 25, 20.3

Cancel OK

Figure 12: Patient data can be entered manually.

**Example Excel Format**

All column names are case sensitive

Missing values should be left blank.

P_ID	age	start_date	year_visit	psa	gleason_sum
10	62.30	2016-02-21	0.00	5.70	6.00
10	62.30	2016-02-21	0.50	NA	NA
10	62.30	2016-02-21	1.00	12.00	6.00
10	62.30	2016-02-21	1.50	8.50	NA
10	62.30	2016-02-21	2.00	15.00	NA
10	62.30	2016-02-21	2.50	NA	6.00
10	62.30	2016-02-21	3.00	25.00	NA
10	62.30	2016-02-21	3.50	20.30	NA

**Description**

**P\_ID** is the ID of the patient and should be a number. Missing values are not allowed.

**age** is the age (years) of the patient when patient started AS. Missing values are not allowed.

**start\_date** is the date on which patient started AS in yyyy-mm-dd format. Missing values are not allowed.

**year\_visit** is the follow-up time (years) since patient started AS, on which either PSA was measured or a biopsy was conducted. Missing values are not allowed.

**psa** is the PSA (ng/mL) at the follow-up time. Missing values should be left blank.

**gleason\_sum** is the Gleason sum (maximum 10) at the follow-up time. Missing values should be left blank.

Download Example File

Figure 13: Patient data can be uploaded via Excel sheets. Example Excel sheet format is provided within the web-application. In addition, users can download an Excel template to fill patient data.

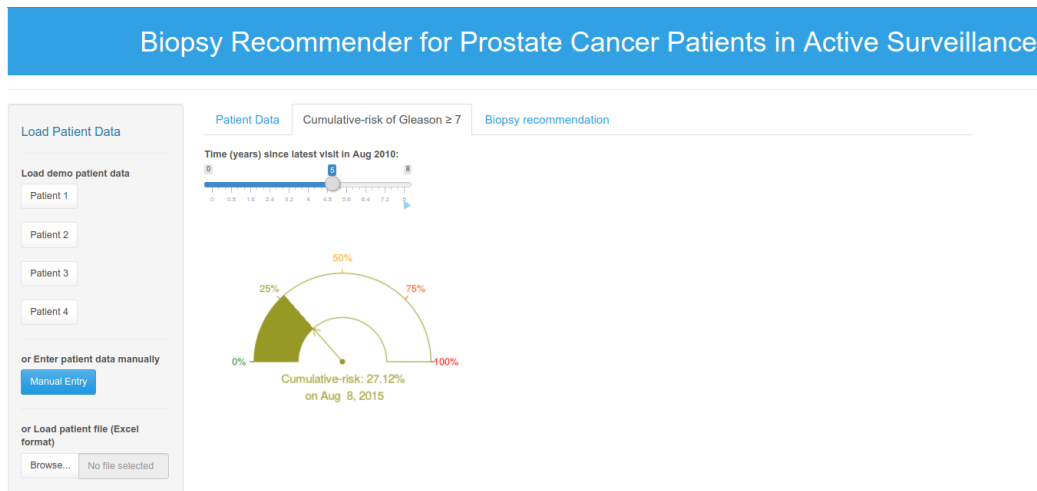


Figure 14: Second tab panel provides patient's personalized cumulative-risk of Gleason  $\geq 7$  since his latest biopsy.

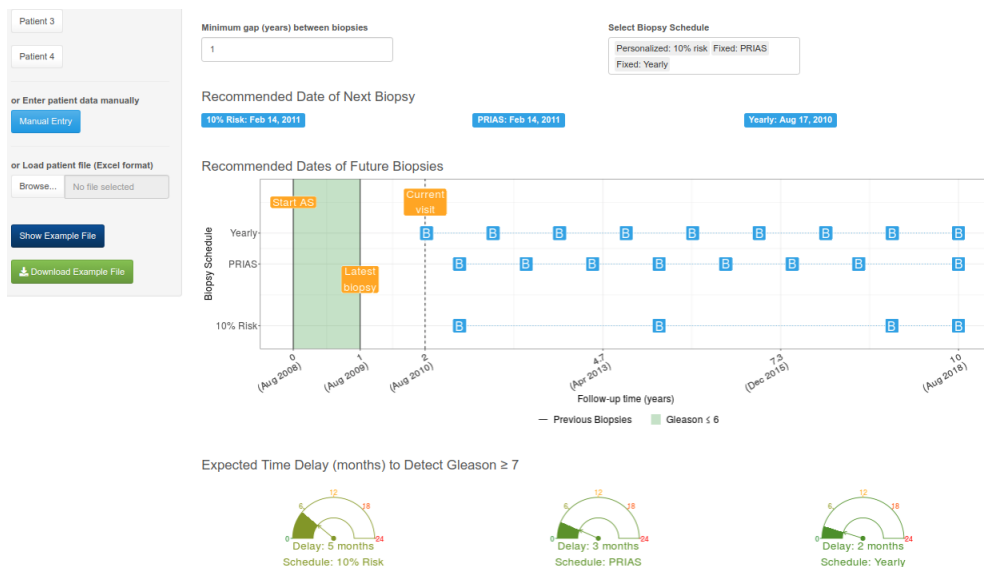


Figure 15: Third tab panel provides personalized and fixed biopsy schedule options as well as the expected time delay in detection of Gleason  $\geq 7$  for each of the schedules.

## 147 Appendix E. Source Code

148 The R code for fitting the joint model to the PRIAS dataset, is at [https://github.com/anirudhtomer/prias/tree/master/src/clinical\\_gap3](https://github.com/anirudhtomer/prias/tree/master/src/clinical_gap3). We  
149 refer to this location as ‘R\_HOME’ in the rest of this document.  
150

### 151 *Appendix E.1. Fitting the Joint Model to the PRIAS dataset*

152 **Accessing the dataset:** The PRIAS dataset is not openly accessible.  
153 However, access to the database can be requested via the contact links at  
154 [www.prias-project.org](http://www.prias-project.org).  
155

156 **Formatting the dataset:** This dataset however is in the so-called wide  
157 format and also requires removal of incorrect entries. This can be done via  
158 the R script `R_HOME/dataset_cleaning.R`. This will lead to two R objects,  
159 namely ‘`prias_final.id`’ and ‘`prias_long_final`’. The ‘`prias_final.id`’ object con-  
160 tains information about time of reclassification for PRIAS patients. The  
161 ‘`prias_long_final`’ object contains longitudinal PSA measurements, the time  
162 of biopsies and results of biopsies.  
163

164 **Fitting the joint model:** We use a joint model for time to event and  
165 longitudinal data to model the evolution of PSA measurements over time,  
166 and to simultaneously model their association with the risk of reclassification.  
167 The R package we use for this purpose is called **JMbayes** ([https://cran.r-](https://cran.r-project.org/web/packages/JMbayes/JMbayes.pdf)  
168 [project.org/web/packages/JMbayes/JMbayes.pdf](https://cran.r-project.org/web/packages/JMbayes/JMbayes.pdf)). The API we use, how-  
169 ever, are currently not hosted on CRAN, and can be found here: [https:](https://github.com/anirudhtomer/JMbayes)  
170 [//github.com/anirudhtomer/JMbayes](https://github.com/anirudhtomer/JMbayes). The joint model can be fitted via  
171 the script `R_HOME/analysis.R`. It takes roughly 6 hours to run on an Intel  
172 core-i5 machine with 4 cores, and 8GB of RAM.

173 The graphs presented in the main manuscript, and the supplementary  
174 material can be generated by the scripts in `R_HOME/plots/`.

### 175 *Appendix E.2. Validation of Predictions of Reclassification*

176 Validations can be done using the script `R_HOME/auc_brier/auc_prederr_`  
177 `no_dre.R`. For external validation access to GAP3 database is required.

### 178 *Appendix E.3. Creating Personalized Schedules of Biopsies*

179 Once a joint model is fitted to the PRIAS dataset, personalized schedules  
180 of biopsies based on risk of reclassification for new patients can be devel-

181 oped using the script `R_HOME/compareSchedules.R`. This script also pro-  
182 vides fixed biopsy schedules for the patients. In addition with each schedule,  
183 the expected delay in detection of reclassification is also provided.

184 *Appendix E.4. Source Code for Web Application*

185     Source for the shiny web application which provides biopsy schedules for  
186 patients can be found at `R_HOME/shinyapp`

- 187 1. Epstein JI, Egevad L, Amin MB, Delahunt B, Srigley JR, Humphrey PA.  
 188 The 2014 international society of urological pathology (isup) consensus  
 189 conference on gleason grading of prostatic carcinoma. *The American*  
 190 *journal of surgical pathology* 2016;40(2):244–52.
- 191 2. Pearson JD, Morrell CH, Landis PK, Carter HB, Brant LJ. Mixed-effects  
 192 regression models for studying the natural history of prostate disease.  
 193 *Statistics in Medicine* 1994;13(5-7):587–601.
- 194 3. Lin H, McCulloch CE, Turnbull BW, Slate EH, Clark LC. A latent  
 195 class mixed model for analysing biomarker trajectories with irregularly  
 196 scheduled observations. *Statistics in Medicine* 2000;19(10):1303–18.
- 197 4. De Boor C. A practical guide to splines; vol. 27. Springer-Verlag New  
 198 York; 1978.
- 199 5. Eilers PH, Marx BD. Flexible smoothing with B-splines and penalties.  
 200 *Statistical Science* 1996;11(2):89–121.
- 201 6. Turnbull BW. The empirical distribution function with arbitrarily  
 202 grouped, censored and truncated data. *Journal of the Royal Statistical*  
 203 *Society Series B (Methodological)* 1976;38(3):290–5.
- 204 7. Bruinsma SM, Zhang L, Roobol MJ, Bangma CH, Steyerberg EW,  
 205 Nieboer D, Van Hemelrijck M, consortium MFGAPPCASG, Trock B,  
 206 Ehdaie B, et al. The movember foundation’s gap3 cohort: a profile of the  
 207 largest global prostate cancer active surveillance database to date. *BJU*  
 208 *international* 2018;121(5):737–44.
- 209 8. Rizopoulos D. The R package JMbayer for fitting joint models for lon-  
 210 gitudinal and time-to-event data using MCMC. *Journal of Statistical*  
 211 *Software* 2016;72(7):1–46.
- 212 9. Rizopoulos D, Molenberghs G, Lesaffre EM. Dynamic predictions with  
 213 time-dependent covariates in survival analysis using joint modeling and  
 214 landmarking. *Biometrical Journal* 2017;59(6):1261–76.